# Zener Polaron Ordering Variants Induced by *A*-Site Ordering in Half-Doped Manganites

A. Daoud-Aladine,[1] C. Perca,[2] L. Pinsard-Gaudart,[2] and J. Rodríguez-Carvajal[3]

[1]*ISIS Facility, Rutherford Appleton Laboratory-CCLRC, Chilton, Didcot, Oxfordshire, OX11 0QX, United Kingdom*
[2]*Laboratoire de Physico-Chimie de l'Etat Solide, Université Paris Sud, Bâtiment 414, 91405 Orsay, France*
[3]*Institut Laue Langevin, 6 rue Jules Horowitz, BP 156, 38042 Grenoble Cedex 9, France*

(Received 22 August 2007; revised manuscript received 19 May 2008; published 15 October 2008)

We have studied the magnetism of the half-doped charge ordered manganite $YBaMn_2O_6$. A formation of ferromagnetic plaquettes of four Mn atoms in the charge ordered phase below $T_{CO} \sim 480$ K is inferred from high temperature magnetic susceptibility data and the magnetic structure, as determined by neutron powder diffraction at $T = 1.5$ K. The results indicate that new fourfold Mn paramagnetic units form between $T_N < T < T_{CO}$, and that they order in a noncollinear mode below $T_N = 190$ K. The magnetism of $YBaMn_2O_6$ is consistent with what is expected from the Zener polarons ordering picture of the charge ordering phenomenon in manganites [A. Daoud-Aladine *et al.*, Phys. Rev. Lett. **89**, 097205 (2002)].

DOI: 10.1103/PhysRevLett.101.166404 PACS numbers: 71.30.+h, 61.05.F−, 75.10.−b, 75.47.Lx

Charge ordering (CO) is a fundamental phenomenon in transition metal oxides which occurs in two famous materials: the $Mn^{3+}/Mn^{4+}$ mixed-valent $R_{1/2}Ca_{1/2}MnO_3$ half-doped manganites ($R$ denotes rare-earth-metal element, Y or La) and magnetite $Fe_3O_4$. Microscopically, CO was originally described as a ionic ordering process, which is nowadays severely called into question [1]. In the manganite, $Mn^{3+}/Mn^{4+}$ CO actually reflects the orbital ordering (OO) on $Mn^{3+}$ ions driven cooperative Jahn-Teller (JT) distortions on $Mn^{+3}O_6$. This concomitant CO/OO explained several aspects of the half-doped manganites' structural and magnetic properties, especially the fact that CO is not a simple $Mn^{3+}/Mn^{4+}$ rock-salt-type order trivially driven by Coulomb repulsion, and how the CO/OO phenomena is connected to the so-called *C*-*E*-type magnetic order (stacking of *C*- and *E*-type structures) [2] by the superexchange (SE) theory [3]. Since the seminal work of [2,3], $R_{1/2}Ca_{1/2}MnO_3$ manganites are said to have a *C*-*E*-type ground state which describes not only the ordering of the Mn spins but also the presumably consistent ordering of the $Mn^{3+}$ and $Mn^{4+}$ charges, the $Mn^{+3}$ orbitals, and associated JT distortions. In the past decade, the validity of the *C*-*E* model and the real presence of CO, as deducible by high-resolution powder diffraction [4,5], was severely disputed by several other experimental techniques [6–8], which all conclude for a much smaller $Mn^{3.5+\delta}/Mn^{3.5-\delta}$ disproportionate setting $\delta < 0.04$ as an upper limit recently quantified as [9].

Ionic CO is disputed in $R_{1/2}Ca_{1/2}MnO_3$, but it has been recently reported in less known charge ordered manganites: the novel *A*-site ordered $RBaMn_2O_6$-type charge ordered materials [10]. These compounds are also half-doped manganites with the same formal 1:1 $Mn^{3+}/Mn^{4+}$ ratio as prototype $R_{1/2}Ca_{1/2}MnO_3$ materials, the only difference being that the $A = R$ (rare-earth metal) and $A' =$ Ba cations are ordered on the $A$ site of the $ABO_3$ perovskite structure, which doubles the chemical formulas as $AA'Mn_2O_6$. *A*-site ordering essentially induces exceptionally high CO transition temperatures ($T_{CO}$), but the transport and magnetic *macroscopic* properties are overall very analogous to that of prototype $R_{1/2}Ca_{1/2}MnO_3$, indicating that the *A*-site cations do not fundamentally change the CO phenomena taking place on the Mn pseudocubic sublattice.

The first models picturing the ground state of these compounds [11,12] were drawn in analogy to the *C*-*E*-type model of $R_{1/2}Ca_{1/2}MnO_3$ manganites [2,3] but are phenomenologically different. The original *C*-*E*-type ground state applies to *all* the $R_{1/2}Ca_{1/2}MnO_3$ compounds, but different models were proposed for different materials, as shown in Fig. 1(a) for $YBaMn_2O_6$ [13] and Fig. 1(b) for $TbBaMn_2O_6$ [14]. It was emphasized that all these models have in common the recovery of a rock-salt-type $Mn^{3+}/Mn^{4+}$ charge order absent in $R_{1/2}Ca_{1/2}MnO_3$. $TbBaMn_2O_6$ would even manifest charge and orbital rearrangements as function of temperature never observed in $R_{1/2}Ca_{1/2}MnO_3$ compounds [14]. In fact, the powder diffraction results of Ref. [14] contradict the transmission electron microscopy (TEM) experiments of Ref. [11]. In Ref. [14], the rock-salt order is said to be preserved up to 473 K, but TEM [11] evidences the appearance of superlattice reflections interpreted as a disruption of the rock-salt order just above $T_N = 200$ K [11]. The TEM superlattice reflections are invisible in powder diffraction, which reports another high temperature orbital reordering transition at $T_s = 96\,^{\circ}$C between the presupposed antiferro-orbital ground state [Fig. 1(b)] and a ferro-orbital order [Fig. 1(a)].

Contradictions in interpretation are not surprising considering that the exact structure of $R_{1/2}Ca_{1/2}MnO_3$-type compounds remains unsolved to date. The majority of works still prefer the original structural symmetry of the *C*-*E* model with a Mn site-centered charge distribution [5–7], and only a few recent results [15,16] back up the alternative Zener polaron (ZP) ordering model [8] related to a Mn-Mn bond-centered charge distribution [17]. In such controversial context, the previous structural results

 

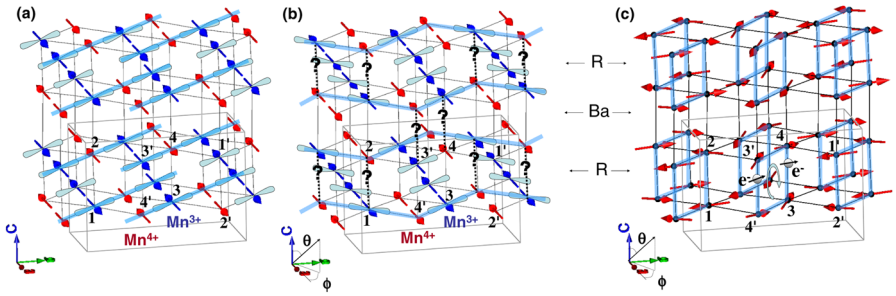


FIG. 1 (color online). Possible ground states of $R\mathrm{BaMn_2O_6}$. Thick blue lines highlight the ferromagnetic spin arrangements. (a) Rock-salt $\mathrm{Mn^{3+}/Mn^{4+}}$ charge order with a ferro-orbital order on the $\mathrm{Mn^{3+}}$ ions, and an expected $C$-type magnetic structure. (b) Antiferro-orbital rock-salt $\mathrm{Mn^{3+}/Mn^{4+}}$ charge order, which has for characteristic, $C$-$E$-like ferromagnetic zizags of $\mathrm{Mn^{4+}}$ and orbitally ordered $\mathrm{Mn^{3+}}$ ions similar to prototype $R_{1/2}D_{1/2}\mathrm{MnO_3}$. Bonds labeled by question marks are not expected to be ferromagnetic and, hence, they are frustrated. (c) Magnetic structure model of $\mathrm{YBaMn_2O_6}$ corresponding to the relaxed ZP ordering model of Table I.

obtained by powder diffraction on $R\mathrm{BaMn_2O_6}$-type materials are not guaranteeing the validity or uniqueness of the proposed ionic CO/OO models in $R\mathrm{BaMn_2O_6}$ [11,12,14]. They only indicate that a very different OO phenomenon is induced by the $A$-site ordering. Any type of $\mathrm{MnO_6}$ distortions (JT or other type) responsible for CO are *a fortiori* more difficult to infer from powder diffraction on $R\mathrm{BaMn_2}2\mathrm{O_6}$ because these compounds already show a strong off-centering of the Mn atoms [18].

Supporting our doubts, the SE theory [3] does not apply very well to $R\mathrm{BaMn_2O_6}$. According to the rules for $\mathrm{Mn^{3+}/Mn^{4+}}$ SE, the ferro-orbital order of $\mathrm{YBaMn_2O_6}$ [Fig. 1(a)], as deduced from neutron powder diffraction (NPD) [13], *must* associate to a $C$-type magnetic arrangement. However, no low temperature NPD data are shown, which could confirm this simple prediction. In fact, our NPD experiments show that the magnetic scattering is essentially the same in $\mathrm{YBaMn_2O_6}$ and $\mathrm{TbBaMn_2O_6}$ [11] (above the Tb ordering temperature), which steadily implies no fundamental reason to distinguish the ground state of $\mathrm{YBaMn_2O_6}$ from that of $\mathrm{TbBaMn_2O_6}$. Finally, the $\mathrm{TbBaMn_2O_6}$ model [Fig. 1(b)] shows dubious signs of magnetic frustration. Unlike the original $C$-$E$ model of $R_{1/2}\mathrm{Ca}_{1/2}\mathrm{MnO_3}$, the CO/OO pattern shows now frustrated bonds incompatible with the presupposed collinearity of the $C$-$E$-like structure. Such frustration is doubly surprising, since $R\mathrm{BaMn_2O_6}$ shows resolution limited magnetic Bragg peaks in NPD and, therefore, a much better established magnetic order than prototype $\mathrm{La}_{1/2}\mathrm{Ca}_{1/2}\mathrm{MnO_3}$ [4].

In this Letter, we show that the $C$-$E$-like magnetic model of $R\mathrm{BaMn_2O_6}$ [Ref. [11] and Fig. 1(b) herein] is not correct. We present results on $\mathrm{YBaMn_2O_6}$, in which no complications arise from the ordering of a magnetic $A$-site cation, as observed in $\mathrm{TbBaMn_2O_6}$. The results of our fit of the NPD data collected at $T = 1.5$ K on the instrument DMC instrument of PSI ($\lambda = 2.47$ Å) are shown in Table I and Fig. 2 [19]. We used the program FULLPROF and its new options permitting the determination of magnetic structures by simulated annealing [20,21]. The procedure allowed us to obtain another solution as a potentially good starting model, in addition to the previously proposed $C$-$E$-like model [11]. The stability and reliability of constrained versions of these models were compared by using Rietveld refinements summarized in Table I and Fig. 2 [19]. They demonstrate that the $C$-$E$-like structure [11] [Fig. 1(b)] is a false minimum, and the new model [Fig. 1(c)] shows much better agreement.

There is no $\mathrm{Mn^{3+}/Mn^{4+}}$ CO/OO configuration that can explain the obtained magnetic structure with SE interactions. However, in analogy to the "ZP ordering" [8], we could rather reconsider the location of the extra $\mathrm{Mn^{3+}}e_g$ charge beyond the atomic level as follows. In Ref. [8] ZPs were proposed to be ferromagnetic Mn pairs, each of which are trapping and sharing one $e_g$ charge. The Mn pairs are ferromagnetic because the trapped charge participates to the double exchange (DE) mechanisms [8]. The unexpected presence of ferromagnetic plaquettes can be taken here as a signature for an ordering of ZPs of four Mn (4Mn ZP) in which each ZP traps $2e_g$ charges delocalized over Mn square plaquettes in $\mathrm{YBaMn_2O_6}$ [Fig. 1(c)].

Here, we invoke ZP ordering as a new phenomenology more than a proper theory of CO, and, as in Ref. [8], our argument mostly refers to mechanisms for "ZP formation" advanced in the context of the physics of colossal magnetoresistive (CMR) manganites [22,23] and apparently independent from the CO problem. In Refs. [22,23], Zhou and Goodenough have experimentally confirmed the existence of a ZP formation in CMR materials through a set of indirect macroscopic and thermodynamic measurements [23]. *In parallel*, the existence of two such manganese ZPs (2Mn ZP) in charge ordered $R_{1/2}\mathrm{Ca}_{1/2}\mathrm{MnO_3}$ was deferred from the structural distortions of $\mathrm{Pr}_{0.60}\mathrm{Ca}_{0.40}\mathrm{MnO_3}$ [8]. The repeated motifs are pairs of $\mathrm{MnO_6}$, within which the elongations, the opening of the Mn-O-Mn angle, and the off-centering of the Mn atoms are all consistent with a strengthening of the ferromagnetic DE interaction within 2Mn Zener pairs [8,16].

Reference [8] establishes a *heuristic* connection between the CO and CMR physics, which promotes the

TABLE I. Refinement of the magnetic structure of $YBaMn_2O_6$. The positions the Mn atoms in the unit cell ($\sqrt{2}a_p$, $2\sqrt{2}a_p$, $2a_p$) are $Mn_1$ (0.261 40, 0.121 78, 0.256 41), $Mn_2$ (0.269 19, 0.127 46, 0.739 27), $Mn_3$ (0.236 67, 0.624 86, 0.254 90), $Mn_4$ (0.234 98, 0.628 06, 0.739 85). $Mn_{i'}$ is related to $Mn_i$ by inversion. Magnetic moments in any cell indexed by $\mathbf{R}_n$ are $\mathbf{m}_{ni} = \mathbf{S}_i(-1)^{\mathbf{k}\cdot\mathbf{R}_n}$, where $\mathbf{k} = (1/2, 0, 1/2)$ is the propagation vector of the magnetic structure. The Mn atom's positions and the spherical coordinate system defining $\phi$ and $\theta$ are shown Fig. 1. The unconstrained model (third column) converges, keeping spin directions close to the constrained model. The better fit indicates that ferromagnetic plaquettes of the constrained model are in reality slightly canted.

| *C-E*-like model (not converging) | Constrained 4Mn ZP order | Unconstrained 4Mn ZP order |
|---|---|---|
| | Constraints | |
| $\mathbf{S}_{i'} = -\mathbf{S}_i$ | $\mathbf{S}_{i'} = \mathbf{S}_i$ | $\mathbf{S}_{i'} = \mathbf{S}_i$ |
| $S_1 = S_3 = m$ | $S_1 = S_2 =$ | $S_1 = S_2 =$ |
| $S_2 = S_4 = m'$ | $S_3 = S_4 = m$ | $S_3 = S_4 = m$ |
| $\phi_1 = \phi_2 = \phi_3 = \phi$ | $\phi_1 = \phi_2 = \phi$ | All $\phi_i$ |
| $\phi_4 = \phi + 180$ | $\phi_3 = \phi_4 = \phi'$ | And $\theta_i$ |
| All $\theta_i = 90$ | All $\theta_i = 90$; | Free |
| | Refinement results | |
| $m = 3.22(3)$ | $m = 3.05(2)$ | $m = 3.06(3)$ |
| $m' = 2.84(3)$ | $\phi = 225(1)$ | $\phi_1 = 211(5)$ $\theta_1 = 88(7)$ |
| $\phi = 5(5)$ | $\phi' = 143(2)$ | $\phi_2 = 239(5)$ $\theta_2 = 105(5)$ |
| | | $\phi_3 = 145(6)$ $\theta_3 = 87(6)$ |
| | | $\phi_4 = 147(5)$ $\theta_4 = 84(6)$ |
| | Agreement factors ($\chi^2$, $R_{\text{Bragg}}$) | |
| $\chi^2 = 102$ | $\chi^2 = 77.0$ | $\chi^2 = 71.8$ |
| $R_{\text{nuclear}} = 2.21\%$ | $R_{\text{nuclear}} = 2.19\%$ | $R_{\text{nuclear}} = 2.21\%$ |
| $R_{\text{magnetic}} = 8.89\%$ | $R_{\text{magnetic}} = 7.13\%$ | $R_{\text{magnetic}} = 5.50\%$ |

existence of *local forms* of DE. In the past, several "model-band" theories of the *C-E* state claimed that they could counterintuitively predict the magnetic structure of $R_{1/2}Ca_{1/2}MnO_3$ without CO (see for instance Ref. [24], and Ref. [25] for a review). The ZP ordering phenomenology similarly stresses the importance of the DE mechanism in the CO physics, but it also stresses the considered localization mechanisms of the charges participating in the DE process that could be more complicated than simple JT distortions. The 2Mn ZP ordered structure [8] suggests a localization essentially achieved by *local* modulations of the Mn-O-Mn angle, which are generally ignored by most band theories. The effect of such distortion in charge order materials becomes apparent in *ab initio* calculations [1,26].

Returning now to the phenomenological description of the magnetic properties of $YBaMn_2O_6$, we confirm the 4Mn ZP order scenario by comparing its *paramagnetic* susceptibility with that of $Y_{1/2}Ca_{1/2}MnO_3$ [8]. Figure 3 shows our measurement of $YBaMn_2O_6$ with a SQUID (Quantum Design) magnetometer. It looks qualitatively very similar to that of $Y_{1/2}Ca_{1/2}MnO_3$ (Fig. 3 of Ref. [8]). Both $1/\chi(T)$ curves show two distinct asymptotic Curie-Weiss behaviors in the two different charge ordered and charge disordered paramagnetic states, associated with two different effective moments. The CO transition actually occurs in two steps in $YBaMn_2O_6$ ($T_{C1} = 480$ K and $T_{C2} = 520$ K). $YBaMn_2O_6$ shows the strongest change of effective moments amongst all the few charge ordered manganates [8,27,28]. For spin only contributions, $\mu^2 = 4S(S+1)$, where $S = n \times \frac{1}{2}$ counts the number $n$ of unpaired electrons in each paramagnetic entity considered. Above $T_{C2} \sim 520$ K and as shown in Fig. 3, the experimental value corresponds well to a mixture of high spin $Mn^{3+}(S = 2)$ and $Mn^{4+}(S = 3/2)$ ions ($\mu_{\text{eff}}^{\text{th}} = \sqrt{1/2\mu^2_{Mn^{3+}} + 1/2\mu^2_{Mn^{4+}}} = 4.41\mu_b$). Possible arrangements of ZPs have $\mu_{\text{eff}} = \sqrt{c\mu^2_{\text{ZP}}}$, taking $c = 1/2$ and $1/4$ for 2Mn ZP ($S = 7/2$) and 4Mn ZP ($S = 7$) orders, respectively. Below $T_{C1}$, the experimental value increases to a value in remarkable quantitative agreement with a 4Mn ZP order ($\mu_{\text{eff}}^{\text{th}} = 7.48\mu_b$).

In summary, instead of ionic CO, we advance ZP ordering as a consistent phenomenology supported by a handful of puzzling experimental results comprising now the structure of $Pr_{0.60}Ca_{0.40}MnO_3$ [8], the magnetic structure of $YBaMn_2O_6$ [Fig. 1(c)], and few susceptibility results

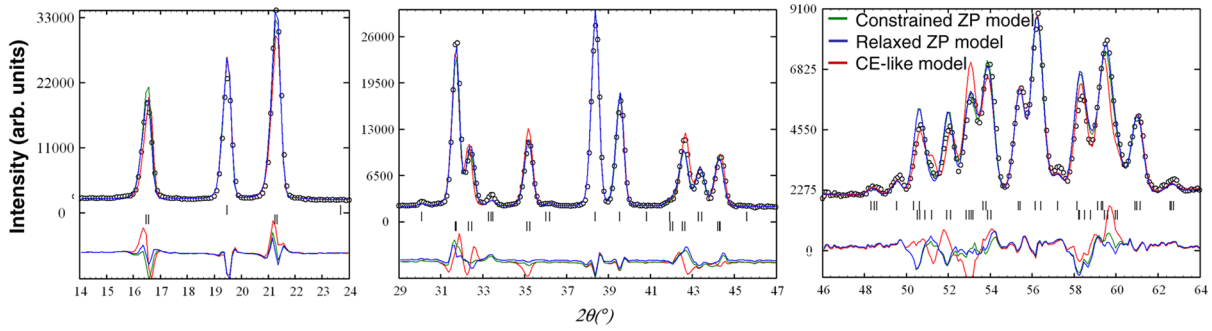


FIG. 2 (color online). Portions of the Rietveld refinements of the NPD pattern of $YBaMn_2O_6$ at $T = 1.5$ K. Nuclear and magnetic Bragg peaks are expected at positions given by the upper and lower ticks, respectively. The curves fitting the data points (circles) and the difference curves between the data and the model are shown for different models. The better agreement of the ZP model is mainly reflected by a better intensity agreement of few clusters of magnetic reflections at 16°, 21°, 32°, 51–54°, and 60°. The relaxation of the constraints essentially improves the fit of the peaks at 31° and 60°.

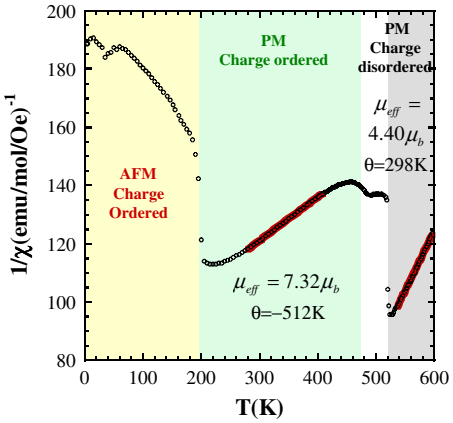


FIG. 3 (color online). Inverse of magnetic susceptibility versus temperature in $YBaMn_2O_6$, collected under an applied magnetic field of 1000 Oe. The thick red lines show the two paramagnetic (PM) temperature ranges in which data follow an asymptotic Curie-Weiss behavior.

[8,27,28]. Previous works on $RBaMn_2O_6$ materials have insisted on the recovery of a rock-salt-like ionic CO [12–14], but no clear microscopic picture has been advanced explaining why this is true.

With the ZP ordering interpretation, we describe a far more dramatic influence of the *A*-site ordering on the CO phenomenon. First, we are implicitly revealing how different cooperative polaronic distortions are adapting to the specificities of the host crystal structures, since they form 4Mn ZPs in $YBaMn_2O_6$ instead of 2Mn ZPs. The 4Mn ZP order of Fig. 1(c) interestingly reflects a quasi-2D charge order in $YBaMn_2O_6$, because the $e_g$ electrons trapped in the 4Mn ZPs preferably surround the small *R* cation. $RBaMn_2O_6$-type materials are in this sense similar to layered manganites, in which the reduced dimensionality of the crystal structure also gives high CO transition temperatures. $R_{1/2}Ca_{1/2}MnO_3$ accommodate the CO process of 2Mn ZPs which appears more 3D. In *A*-site disordered $R_{1/2}Ba_{1/2}MnO_3$, the CO and antiferromagnetic (AFM) properties are replaced by low temperature glassy magnetic properties [10], which probably reflects the impossibility for large ZPs to form and/or order properly. The comparison of the *A*-site ordered and *A*-site disordered half-doped manganites therefore shows that the ZP ordering interpretation(s) gives more consistent pictures for the CO process than ionic CO, which accounts better for the different crystal chemistry of different materials.

We acknowledge S. McLain, P. Radaelli, and J. D. M. Champion for critical readings of the manuscript. Neutron diffraction experiments were performed at the SINQ, Paul Scherrer Institute, Villigen, Switzerland, and at the LLB, CEA Saclay, France, neutron sources.

[1] M. Coey, Nature (London) **430**, 155 (2004).
[2] E. O. Wollan and W. C. Koehler, Phys. Rev. **100**, 545 (1955).
[3] J. B. Goodenough, Phys. Rev. **100**, 564 (1955).
[4] P. Radaelli, D. Cox, M. Marezio, and S. Cheong, Phys. Rev. B **55**, 3015 (1997).
[5] R. J. Goff and J. P. Attfield, Phys. Rev. B **70**, 140404 (2004).
[6] S. Grenier *et al.*, Phys. Rev. B **69**, 134419 (2004).
[7] E. E. Rodriguez *et al.*, Phys. Rev. B **71**, 104430 (2005).
[8] A. Daoud-Aladine *et al.*, Phys. Rev. Lett. **89**, 097205 (2002).
[9] J. C. Loudon *et al.*, Phys. Rev. Lett. **99**, 237205 (2007).
[10] D. Akahoshi *et al.*, Phys. Rev. Lett. **90**, 177203 (2003).
[11] T. Arima *et al.*, Phys. Rev. B **66**, 140408(R) (2002).
[12] A. Williams and J. Attfield, Phys. Rev. B **66**, 220405(R) (2002).
[13] A. J. Williams and J. P. Attfield, Phys. Rev. B **72**, 024436 (2005).
[14] A. J. Williams, J. P. Attfield, and S. A. T. Redfern, Phys. Rev. B **72**, 184426 (2005).
[15] M. Giot, A. Pautrat, O. Perez, C. Simon, M. Nevriva, and M. Hervieu, Solid State Sci. **8**, 1414 (2006).
[16] L. Wu, R. F. Klie, Y. Zhu, and C. Jooss, Phys. Rev. B **76**, 174210 (2007).
[17] D. Effremov, J. Van Den Brink, and D. Khomskii, Nature Mater. **3**, 853 (2004).
[18] In our structural refinements, we have systematically used restraints on the Mn-O bond distances: this confirms the impossibility to clearly distinguish between competing CO ordering models in this material. Results will be published elsewhere.
[19] Constraints on the magnetic parameters are necessary to avoid divergence. All other structural and profile parameters are also preferably and carefully fixed to known values. The average atomic positions were obtained from combined refinements of laboratory x-ray diffraction data (monochromatic Cu $K\alpha_1$ radiation) and NPD data from the 3T2 NPD instrument at the LLB source ($\lambda$ = 1.22 Å), CEA, France. The cell parameters (monoclinic, $a$ = 5.521 Å, $b$ = 11.029 Å, $c$ = 7.579 Å, $\beta$ = 90.34°) used for treating the presented DMC data were taken and fixed from the refinement of $T$ = 15 K high-resolution neutron diffraction data ($\lambda$ = 1.493 Å) collected on the HRPT diffractometer, SINQ source, PSI, Switzerland.
[20] S. Kirpatrick, C. Gelatt, and M. Vecci, Science **220**, 671 (1983).
[21] J. Rodríguez-Carvajal, Mater. Sci. Forum **378–381**, 268 (2001).
[22] J. Zhou and J. Goodenough, Phys. Rev. B **62**, 3834 (2000).
[23] J. B. Goodenough and S. L. Cooper, *Localized to Itinerant Electronic Transition in Perovskite Oxides. Structure and Bonding*, edited by J. B. Goodenough (Springer, New York, 2001).
[24] I. V. Solovyev and K. Terakura, Phys. Rev. Lett. **83**, 2825 (1999).
[25] E. Dagotto, T. Hotta, and A. Moreo, Phys. Rep. **344**, 1 (2001).
[26] G. Zheng and C. H. Patterson, Phys. Rev. B **67**, 220404 (2003).
[27] C. Frontera *et al.*, Phys. Rev. B **68**, 134408 (2003).
[28] J. J. Hejtmnek *et al.*, J. Appl. Phys. **93**, 7370 (2003).